"Onsager-molecule" approach to liquid structure: The one-component plasma in two and three dimensions

Y. Rosenfeld
Nuclear Research Center Negev, P.O. Box 9001, Beer-Sheva 84190, Israel

D. Levesque and J. J. Weis
Laboratoire de Physique Theorique et Hautes Energies, Universite de Paris–Sud, 91405 Orsay, France
(Received 29 August 1988)

The structure of the strongly coupled uniform one-component plasma (OCP) in two and three dimensions and the density profile of a three-dimensional OCP near a hard wall are calculated by the "Onsager-molecule" approach. We demonstrate that the structure of a strongly coupled plasma can be calculated very accurately (nearly within the simulation uncertainty) by employing only the leading term in the strong-coupling expansion of the bridge function.

I. INTRODUCTION

The pair structure of a fluid of particles interacting by the pair potential $\phi(r)$ is uniquely determined from the simultaneous solution of the Ornstein-Zernike (OZ) equation[1]

$$h(r)=c(r)+\rho\int dr' h(|\mathbf{r}-\mathbf{r}'|)c(\mathbf{r}') \tag{1.1}$$

and the closure relation

$$c(r)=-\beta\phi(r)-\ln[g(r)]+h(r)-B(r)\ . \tag{1.2}$$

Here ρ is the density, β is the inverse temperature $1/k_BT$, $h(r)$ and $c(r)$ denote the pair and direct correlation functions, respectively, and

$$g(r)=h(r)+1\ . \tag{1.3}$$

Equation (1.2) contains the so-called bridge function[1] $B(r)$ which is a unique functional of the pair correlation function $h(r)$, i.e., $B(r)=B\{h(r)\}$. Although it is known in the form of an expansion in highly connected h-bond diagrams,[1,2] the convergence of the expansion is generally too slow for it to be applicable to calculations of the highly correlated dense fluid phase.

Neglect of $B(r)$ in Eq. (1.2) constitutes the hypernetted-chain approximation (HNCA), which is at best qualitative in the strongly correlated phase. The most significant improvement over the HNCA has been obtained by approximating the bridge function in (1.2) by that of hard spheres, the adjustable hard-sphere diameter being determined by imposing consistency between the different routes to the thermodynamic properties. This approach gives quantitative predictions for a variety of potential models and over a wide range of state conditions including the strongly correlated region[3–5] and gives support for some kind of universal behavior of the bridge function at short range.[3,6]

Here we follow a different route which consists of approximating the bridge function by its asymptotic high-density limit (AHDL). It has been shown recently by one of us[7] how the latter can be derived from the AHDL of Eq. (1.2). For plasmas, which we will primarily be concerned with here, the asymptotic strong-coupling state associated with Eqs. (1.1) and (1.2) can be characterized[8] as an "ideal" state (called Onsager state) in which the thermodynamics are given by the sum of the individual contributions of entities called "Onsager atoms" (OA's) and "Onsager molecules" (OM's), which will be defined below. This ideal state is unphysical in the sense that the sum of the excluded volumes of the hard cores of the "molecules" and "atoms" is equal to the volume of the system. However, an expansion about this state is believed to be rapidly convergent over a wide range of coupling parameters of physical interest. Preliminary results for the three-dimensional (3D) one-component plasma (OCP) in a uniform background have indeed shown[7] that this novel theory, which contains no adjustable parameters and is thermodynamically fully consistent, nearly reproduces the pair correlation function near freezing within the statistical error of the computer simulations.

The purpose of the present paper is to present more elaborate numerical results for the 3D OCP as well as results for the thermodynamics and pair structure of the 2D OCP and for the density profile of a nonuniform 3D OCP in the vicinity of a hard wall.

The general formalism leading to the AHDL limit of $B(r)$ is summarized in Sec. II. Explicit expressions for the bridge functions are given in Sec. III. The inherent consistency condition for the bridge functions together with bridge function inequalities is discussed in Sec. IV. In Sec. IV we also present and discuss the numerical solution of Eqs. (1.1) and (1.2) using the AHDL bridge function for the bulk OCP in two and three dimensions [we shall call this the modified hypernetted chain equation (MHNC)]. MHNC results for the OCP near a hard wall are given in Sec. V. Implications of this work and suggestions for further studies are discussed in the concluding section, Sec. VI.

II. ASYMPTOTIC STRONG-COUPLING EXPRESSION FOR THE BRIDGE FUNCTION

In this section we summarize the different steps which lead to the asymptotic strong-coupling limit of the bridge function. To begin with, it is convenient to write the bridge function in the form

$$B(r)=h(r)-c(r)-H(r) , \tag{2.1}$$

where $H(r)$ is the "screening potential" defined by

$$H(r)=\ln[g(r)]+\beta\phi(r) . \tag{2.2}$$

The pair potential of a D-dimensional OCP is

$$\phi(r)=(Ze)^2\phi_D(r) , \tag{2.3a}$$

where

$$\phi_D(r)=\begin{cases}\mathrm{sgn}(D-2)r^{2-D}, & D\neq 0\\ -\ln(r), & D=2\end{cases} \tag{2.3b}$$

and Ze is the charge of an ion. A dimensionless coupling parameter will be defined by

$$\Gamma=\beta(Ze)^2a^{2-D} , \tag{2.4}$$

where a is the ion-sphere (Wigner-Seitz) radius

$$a=[D\Gamma(D/2)/(2\pi^{D/2}\rho)]^{1/D} \tag{2.5}$$

[here $\Gamma(x)$ is the gamma function]. Throughout the remainder of this paper all distances will be expressed in units of a.

In the asymptotic strong-coupling limit (i.e., $\Gamma\to\infty$) the following results have been shown to apply[7-9] (denoting by a superscript ∞ the leading asymptotic large Γ contributions):

$$h^{\infty}(r)=-1, \quad r\leq 2 \tag{2.6a}$$

$$c^{\infty}(r)=c^{\infty}_{\mathrm{HNCA}}(r)+\Delta c^{\infty}(r), \quad r\leq 2 \tag{2.6b}$$

$$c^{\infty}(r)=-H^{\infty}(r)=-\beta\phi(r), \quad r\geq 2 \tag{2.6c}$$

$$B^{\infty}(r)=0, \quad r\geq 2 . \tag{2.6d}$$

Recall[9] that in the asymptotic strong-coupling limit $c^{\infty}(r)$, $-H^{\infty}(r)$, $-\beta\phi(r)$, and $B^{\infty}(r)$ are of order Γ, while $h^{\infty}(r)/\Gamma=0$, so that

$$B^{\infty}(r)=-[c^{\infty}(r)+H^{\infty}(r)] .$$

In Eq. (2.6b), $c^{\infty}_{\mathrm{HNCA}}(r)$ denotes the result of the HNC approximation [i.e., Eq. (1.2) with $B(r)=0$] which can be expressed[9,10] as the electrostatic interaction Ψ of two uniformly charged spheres of unit radius, unit total charge, and separation r,

$$c^{\infty}_{\mathrm{HNCA}}(r)=-\Gamma\Psi(r) . \tag{2.7}$$

The deviation of the asymptotic strong-coupling direct correlation function from its HNCA value is[7]

$$\Delta c^{\infty}(r)=-q\Gamma\omega(r) , \tag{2.8a}$$

where $\omega(r)=\Omega(r)/\Omega(r=0)$, and $\Omega(r)$ is the overlap volume of two D-dimensional spheres of unit radius at separation r. With Z and χ denoting the compressibility factor, $P/\rho k_BT$, and inverse compressibility, $\beta(\partial P/\partial\rho)_T$, respectively, then

$$q=-\lim_{\Gamma\to\infty}[(\chi-2Z)/\Gamma]_{\mathrm{HNCA}} , \tag{2.8b}$$

i.e., q is obtained from the "ion-sphere" approximation to the equation of state, which in strong coupling coincides with the HNC integral equation result for both $B=0$ and for the self-consistent $B(r)$.

To obtain the asymptotic contribution to $H(r)$ it is convenient to express $H(r)$ in the form [derived from the definition of $g(r)$ in the canonical ensemble[11]]

$$H(r)=-\beta\{F_1^{\mathrm{ex}}[r,(N-2)]-F_0^{\mathrm{ex}}[N]\}+\phi(r) . \tag{2.9}$$

Here F_0 is the configurational (excess over ideal gas) free energy of the N-particle system (in a uniform neutralizing background) and $F_1^{\mathrm{ex}}[r,(N-2)]$ is that of the same system but with one pair of particles kept at fixed separation r forming a two-site charge cluster. F_1^{ex} does contain the intramolecular interaction $\phi(r)$, so that $H(r)$ is finite as $r\to 0$.

In the limit $\Gamma\to\infty$ (Refs. 8 and 9)

$$(F_0^{\mathrm{ex}}[N])^{\infty}=Nu_{\mathrm{OA}} , \tag{2.10a}$$

$$(F_1^{\mathrm{ex}}[r,(N-2)])^{\infty}=(N-2)u_{\mathrm{OA}}+u_{\mathrm{OM}}(r) , \tag{2.10b}$$

and

$$H^{\infty}(r)=\beta\phi(r)-\beta u_{\mathrm{OM}}(r)+2\beta u_{\mathrm{OA}} . \tag{2.11}$$

In Eq. (2.10a), u_{OA} is[8,9] the self-energy of an Onsager atom consisting of a point charge at the center of a neutralizing unit sphere having the background charge density. Similarly[8,9] u_{OM} is the self-energy of an Onsager molecule consisting of a pair of ions separated by a distance r in a uniform neutralizing charge cloud of background charge density. The shape of this molecule is determined by the surface on which the electrostatic field vanishes. Onsager molecules have the property to "dissociate" whenever the distance between the two point charges is larger than 2, i.e.,

$$u_{\mathrm{OM}}(r)=2u_{\mathrm{OA}} \quad \text{for } r\geq 2 \tag{2.12}$$

in accord with (2.6c).

An exact calculation of $u_{\mathrm{OM}}(r)$ is straightforward,[12] but has to be done numerically. The corresponding $H^{\infty}(r)$ will be denoted $H_{\mathrm{OM}}(r)$. The fact that $u_{\mathrm{OM}}(r)$ represents an optimal energy bound suggests analytic approximations. In particular, we shall consider the "Onsager smearing bound"[8] (OSB), which satisfies the dissociation property (2.12). In this approximation every molecular point charge is uniformly smeared inside a sphere of radius b (in units of a) which is determined by optimizing the corresponding Onsager bound to u_{OM}. An explicit expression of $H_{\mathrm{OSB}}(r)$ for the 3D OCP can be found in Ref. 8. However, at the present time, no analytic expression for the 2D case is available.

If the radius b is not optimized but taken equal to 1 then[7]

$$H^{\infty}(r)=[H^{\infty}(r)]_{\text{nonoptimized OSB}}$$
$$=\Gamma\Psi(r)=-c^{\infty}_{\text{HNCA}}(r)\ . \tag{2.13}$$

Since these estimates represent decreasingly accurate lower bounds to a free energy, they do obey (as can also be verified by straightforward electrostatic calculation) the following exact inequalities:[7,12]

$$H_{\text{OM}}(r)\le H_{\text{OSB}}(r)\le -c^{\infty}_{\text{HNCA}}(r)\ . \tag{2.14}$$

As a result the corresponding asymptotic bridge functions satisfy

$$B_{\text{OM}}(r)\ge B_{\text{OSB}}(r)\ge -\Delta c^{\infty}(r)\ . \tag{2.15}$$

In the range relevant to the scattering problem of strongly coupling plasmas, $r\gtrsim 1$ [as $g(r\lesssim 1)=0$, in strong coupling], the deviations between the three estimates of $H^{\infty}(r)$ in (2.14) are less than 1%. However, the corresponding deviations in the $B(r)$'s are much larger and may exceed 50%.

The bridge function as obtained from the nonoptimal OSB is universal, i.e., it is the same for all potentials, and equals

$$B_{\text{universal}}(r)=-\Delta c^{\infty}(r)=q\Gamma\omega(r)\ . \tag{2.16}$$

It thus represents the universal component of the strong coupling $B(r)$, which can be conveniently written in the form

$$B_{\text{OM,OSB}}(r)=\lambda_{\text{OM,OSB}}(r)B_{\text{universal}}(r)$$
$$=\lambda_{\text{OM,OSB}}(r)q\Gamma\omega(r)\ . \tag{2.17}$$

The function $\lambda_{\text{OM,OSB}}(r)$, i.e., either $\lambda_{\text{OM}}(r)$ or $\lambda_{\text{OSB}}(r)$, which must obey [cf. (2.15)]

$$\lambda_{\text{OM,OSB}}(r)\ge 1\ , \tag{2.18}$$

represents the deviations of the asymptotic bridge function from its universal part. $B_{\text{universal}}(r)$ always provides an exact lower bound to the asymptotic bridge function.

III. BRIDGE FUNCTIONS FOR STRONGLY COUPLED PLASMAS: EXPLICIT EXPRESSIONS FOR THE ONE-COMPONENT PLASMA IN ONE, TWO, AND THREE DIMENSIONS

The results of Sec. II apply quite generally to a D-dimensional plasma. Here we give explicit expressions for $D=1$, 2, and 3, whenever they are available. They correspond to the range $r\le 2$. We recall that $B^{\infty}(r)=0$ for $r>2$. We define $t=r/2$ (r in units of a).

A. OCP in one dimension: $\phi_D(r)=-r$, $q=\frac{1}{3}$

In one dimension all required expressions can be obtained analytically with the following results (denoting $t=r/2$):

$$H_{\text{OM}}(r)/\Gamma=-(1+t^2)\ , \tag{3.1}$$
$$c^{\infty}_{\text{HNCA}}(r)/\Gamma=\tfrac{2}{3}+2t^2-2t^3/3 \tag{3.2}$$
$$\Delta c^{\infty}(r)/\Gamma=-(1-t)/3\ , \tag{3.3}$$
$$B_{\text{OM}}(r)/\Gamma=\tfrac{2}{3}-t/3-t^2+2t^3/3\ , \tag{3.4}$$
$$\lambda_{\text{OM}}(r)/\Gamma=2+t-2t^2\ . \tag{3.5}$$

B. OCP in three dimensions: $\phi_D(r)=1/r$, $q=\frac{1}{5}$

From the analytical expressions for $\Psi(r)$ and $\omega(r)$ it follows that

$$\Delta c^{\infty}(r)/\Gamma=-(1-3t/2+t^3/2)/5\ , \tag{3.6}$$
$$c^{\infty}_{\text{HNCA}}(r)/\Gamma=-(1.2-2t^2+3t^3/2-t^5/5)\ . \tag{3.7}$$

Results for $H_{\text{OM}}(r)$ and $H_{\text{OSB}}(r)$ are presented in Table I, along with similar results for $D=1$. Note that the Onsager smearing results are very accurate, yet in Fig. 1 we find that the corresponding differences in $\lambda(r)$ are much more pronounced, especially in the region $r>1$ which is

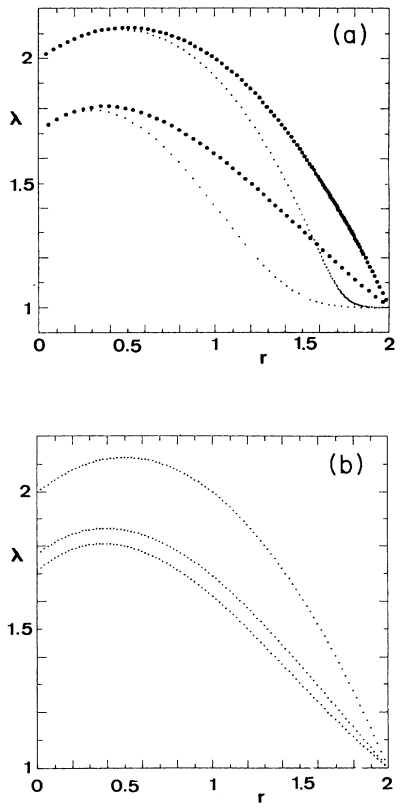

FIG. 1. Asymptotic strong-coupling ratio, $\lambda_{\text{OM,OSB}}(r)=B_{\text{OM,OSB}}(r)/B_{\text{universal}}(r)$, of the bridge function to its universal component for the one-component plasma (see the text). (a) Results of exact Onsager-molecule calculations (large dots) and of the Onsager smearing bound (small dots) for $D=1$ (upper curves) and $D=3$ (lower curves). (b) Exact Onsager-molecule results for $D=1,3$ and the interpolation curve for $D=2$ [Eqs. (3.5), (3.9), and (3.10), respectively].

TABLE I. Screening potential $H(r)$ of the 1D and 3D OCP. H_{OM} denotes the exact Onsager-molecule calculations and H_{OSB} the Onsager smearing bound (see the text).

	$D=3$			$D=1$	
r	H_{OSB}/Γ	H_{OM}/Γ	r	$-H_{OSB}/\Gamma$	$-H_{OM}/\Gamma$
0	1.0573	1.0573	0	1	1
0.2	1.0479	1.0474	0.3171	1.0246	1.0251
$\frac{2}{3}$	0.9619	0.9536	0.5818	1.0817	1.0846
1	0.8555	0.8427	1.0420	1.2592	1.2714
$\frac{4}{3}$	0.7254	0.7171	1.3797	1.4561	1.4759
1.6	0.6222	0.6203	1.7090	1.7148	1.7302
2	$\frac{1}{2}$	$\frac{1}{2}$	2	2	2

the most important from the standpoint of the solution of Eq. (1.2). These results show that the nonuniversal features of $B(r)$ are significant. The function $\lambda_{OM}(r)$ has been fitted by a polynomial of the form

$$\lambda_{OM}(r)=A_0+A_1t+A_2t^2+A_3t^3 . \tag{3.8}$$

The value of A_0 is known exactly from the ion-sphere result for $H^{\infty}(0)$, while $A_1=\omega(t=0)(1-A_0)$. Since we further require that $\lambda_{OM}(t=1)=1$, we are left with one adjustable parameter which we determine by imposing the position t_0 of the maximum of $\lambda_{OM}(t)$. This procedure yields the exact $\lambda_{OM}(t)$ for $D=1$ and turns out to be convenient for determining $\lambda(t)$ in two dimensions where no exact calculations of $\lambda_{OM}(t)$ have yet been obtained. For $D=3$ one has

$$\lambda_{OM}(r)=1.713+1.07t-3.24t^2+1.457t^3 , \tag{3.9}$$

which gives $t_0=0.189$. This fit represents the calculated values[12] for $r\le 1.6$ by better than 2%.

C. OCP in two dimensions: $\phi_D(r)=-\ln(r)$, $q=\frac{1}{4}$

For $D=2$ no exact self-energy calculations for the Onsager molecule are available to us. However, using the procedure described above, we can determine an approximate λ_{OM}:

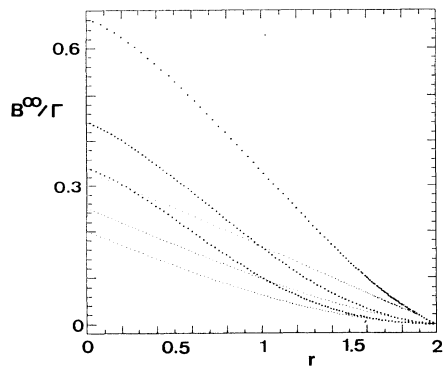

FIG. 2. Asymptotic strong-coupling bridge functions $B_{OM}(r)=\lambda_{OM}(r)B_{universal}(r)$ for $\lambda_{OM}(r)$ given in Fig. 1(a) (large dots), and its universal component $B_{universal}(r)$ (small dots) for the OCP. From top to bottom, $D=1,2,3$.

$$\lambda_{OM}^{approx}(r)=1.773+0.984t-2.818t^2+1.061t^3 , \tag{3.10}$$

where we have used the known values for A_0 and A_1 [see Eqs. (3.1)] and t_0 obtained from interpolation between its values at $D=1$ and 3.

Other asymptotic properties of the 2D OCP are[7]

$$\begin{aligned}
&\beta u_{OA}=-3\Gamma/8,\quad Z^{\infty}=-\Gamma/4,\quad \chi^{\infty}_{HNCA}=-\Gamma/2 ,\\
&c^{\infty}_{HNCA}(0)=-\Gamma/4,\quad \chi^{\infty}=-\Gamma/4,\quad c^{\infty}(0)=-\Gamma/2 ,\\
&H^{\infty}(0)=(0.75-\ln 2)\Gamma\sim 0.0569\Gamma ,\\
&B_{OM}(0)=(\ln 2-0.25)\Gamma\sim 0.443\Gamma ,\\
&\lambda_{OM}(0)=4\ln 2-1\sim 1.773 .
\end{aligned} \tag{3.11}$$

From these values and the analytical expression for the overlap volume function one gets

$$\Delta c^{\infty}(r)/\Gamma=-(2/\pi)[\arccos(t)-t(1-t^2)^{1/2}]/4 . \tag{3.12}$$

The resulting asymptotic bridge functions for $D=1,2,3$ and their universal components are presented in Fig. 2.

IV. NUMERICAL SOLUTION OF THE MODIFIED HNC EQUATION FOR THE BULK OCP IN TWO AND THREE DIMENSIONS

A. Inherent (unimposed) self-consistency

The strong-coupling expression for the bridge function, provided by the Onsager-molecule analysis in Sec. II, is now used as an approximation for the bridge function to solve Eqs. (1.1) and (1.2) for the pair structure at finite Γ. The validity of the approach can and will be established by comparing the pair correlation functions with "exact" simulation results. However, it can be checked directly, without relying on any such outside information, in the following way. When accurate values of $B_{OM}(r)$ are available (as is the case for the 3D OCP), then (2.8) which is a basic ingredient in the derivation of $B_{OM}(r)$, will provide a self-consistency check of the calculations at sufficiently high couplings. If $B(r)=\lambda\Gamma q\omega(r)$ is known only approximately as is presently still the case for the 2D OCP and the OCP near a hard wall then it can be checked to what extent the relation

$$\begin{aligned}
&||c_{MHNC}(r)-c^{\infty}_{HNCA}(r)|-\Delta c^{\infty}(r)|\\
&\qquad\lesssim |c_{HNCA}(r)-c^{\infty}_{HNCA}(r)|
\end{aligned} \tag{4.1}$$

is obeyed. The right-hand side of (4.1) provides a measure for the deviations from true asymptotic behavior. By monitoring to what extent (4.1) is obeyed, and by recalling the inequalitities (2.15), we can even "invert" the problem and use the MHNC results in strong coupling to estimate the Onsager-molecule self-energy.

It should be noted that in Eq. (1.2) only the values of $B(r)$ in the region where $g(r)\neq 0$ (typically for $r>1.3$, in strong coupling) play a role in determining the MHNC results for $g(r)$. Yet our consistency check (2.8), i.e.,

(4.1), strongly emphasizes the region $r<1.3$. Also, a correct trial bridge function [if $B_{\rm OM}(r)$ is not available] should give a solution of the MHNC equation, at finite Γ, that satisfies (2.11) to within entropic contributions to the OCP free energy[7,8] (in particular, for values close to $r=0$).

B. OCP in three dimensions

All MHNC calculations were performed by a method similar to that of Ng (Ref. 13) using 2048 grid points and a grid size of $0.02a$, except for the highest density ($\Gamma=313.6$), where 4096 points were used. The results presented here supplement those given in Ref. 7. Figure 3(a) compares

$$\Delta c(r)/\Gamma=[c(r)-c_{\rm HNCA}(r)]/\Gamma$$

with the theoretical asymptotic value $\Delta c^{\infty}(r)/\Gamma$, employed to derive the bridge function, for $\Gamma=40$, 100, and 313.6. The consistency condition (2.8) and (4.1) is well satisfied even for the lowest value of Γ. Figure 3(b) shows similar results at $\Gamma=100$ but for two expressions of the bridge function, $B_{\rm OM}(r)$ and $B_{\rm universal}(r)$. The consistency

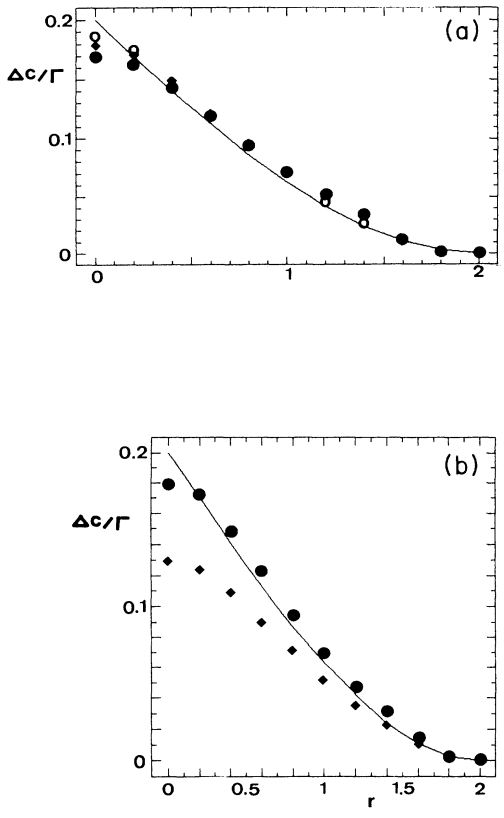

FIG. 3. Modified HNC calculations for the 3D OCP using the Onsager-molecule bridge function. (a) Deviation $\Delta c(r)/\Gamma$, of the direct correlation function from its asymptotic strong-coupling prediction [check of Eq. (4.1)], for $\Gamma=40$ (closed circles), 100 (diamonds), and 313.6 (open circles). (b) Same for $\Gamma=100$ (closed circles) featuring also the results for $B_{\rm universal}(r)$ (diamonds).

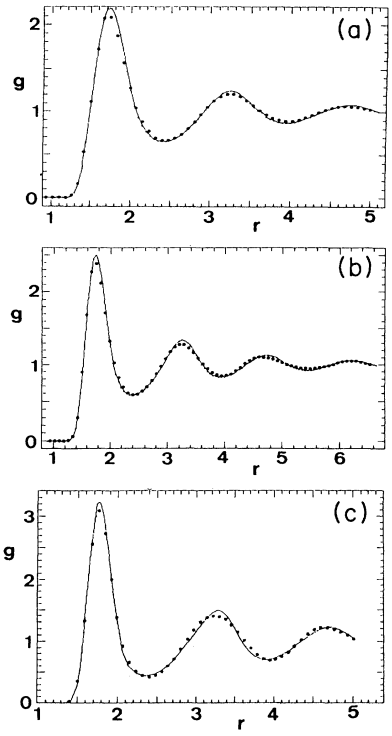

FIG. 4. Radial distribution function $g(r)$, for the 3D one-component plasma. Comparison of the modified HNC calculations using the Onsager-molecule bridge functions $B_{\rm OM}(r)$ (solid lines) with the Monte Carlo results (Refs. 14 and 15) (dots, see text): (a) $\Gamma=110$; (b) $\Gamma=160$; (c) $\Gamma=313.6$.

is seen to be greatly improved by the effect of $\lambda_{\rm OM}(r)$.

The pair distribution function $g(r)$ obtained with $B(r)=B_{\rm OM}(r)$ is compared in Figs. 4(a) and 4(b) with the Monte Carlo calculations[14] for $\Gamma=100$ and 160, and in Fig. 4(c) with the simulations[15] for $\Gamma=314$. The agreement is quite good except for a small shift in the peak positions most visible at the lowest Γ values. Figure 5 com-

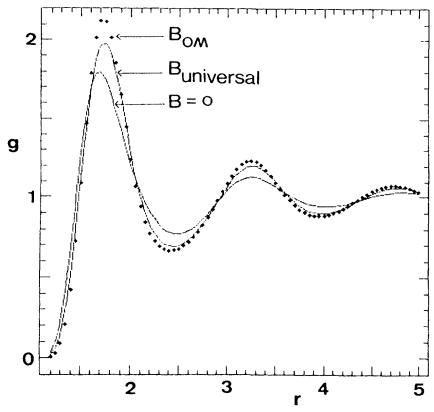

FIG. 5. Radial distribution function $g(r)$, for the 3D one-component plasma for $\Gamma=100$. Results of Eq. (1.2) with $B=0$ (HNC), $B_{\rm universal}$ [Eq. (2.16)], and $B_{\rm OM}$ [Eq. (2.17) with (3.9)].

TABLE II. Internal energy U and inverse compressibility χ of the 3D OCP. The results correspond to Eq. (1.2) with bridge functions $B=0$ (HNC) and B_{OM} [Eq. (2.17) with λ_{OM} given by (3.9)]. The Monte Carlo (MC) results are from Refs. 14 and 15.

	V			χ		
Γ	B_{OM}	MC	HNC	B_{OM}	HNC	MC
1	−0.589	−0.572	−0.570	0.984	0.718	0.730
5	−3.811	−3.757	−3.732	0.247	−0.990	−0.715
10	−8.068	−7.998	−7.935	−1.027	−3.424	−2.619
20	−16.755	−16.673	−16.537	−3.978	−8.626	−6.498
40	−34.350	−34.255	−33.999	−10.538	−19.555	−14.345
60	−52.060	−51.961	−51.597	−17.500	−30.792	−22.235
80	−69.825	−69.725	−69.263	−24.682	−42.195	−30.145
100	−87.625	−87.522	−86.973	−32.007	−53.703	−38.067
120	−105.448	−105.345	−104.713	−39.436	−65.287	−45.997
140	−123.288	−123.188	−122.475	−46.942	−72.929	−53.933
160	−141.141	−141.036	−140.255	−54.510	−88.616	−61.873
200	−176.878	−176.765	−175.856	−69.784	−112.097	−77.764
313.6	−278.498	−278.35	−277.137	−113.783	−179.282	−122.94

pares the $g(r)$'s obtained with three different bridge functions $B_{OM}(r)$, $B_{universal}(r)$, and $B(r)=0$ (HNCA) at $\Gamma=110$. The use of $B_{universal}(r)$ improves already considerably upon the HNCA approximation.

The thermodynamic data, internal energy, and compressibility χ^{-1} are summarized in Table II, and compared with HNCA and Monte Carlo results. The energy is very close to the exact result; however, a systematic deviation of ~ 0.1 seems to occur for $\Gamma \geq 20$. The compressibility is much more sensitive to the input $B(r)$. The use of the Onsager-molecule bridge function greatly improves upon the HNC results at large Γ but does not entirely close the gap with the Monte Carlo results.

C. OCP in two dimensions

In two dimensions Eqs. (1.1) and (1.2) have been solved using the numerical method proposed by Talman[16] and previously applied to the solution of the HNC equation.[17] The number of grid points used was 2048. Except for a greater sensitivity of the results to the input $B(r)$, the trends for the 2D OCP are quite similar to those in three dimensions. Both $\lambda=1$ and λ from Eq. (3.10) substantially improve the HNC results for $g(r)$ from the standpoint of thermodynamic consistency and values for the energy [see Table III, parts (a) and (b)]. The exact compressibility is best reproduced by the choice $\lambda=1$. However, this choice gives a pair correlation function whose peak heights are too low and peak positions shifted to higher values as compared to the simulation results[18] (see Fig. 6). With λ given by (3.10) the peak positions are nearly right but the peak heights are somewhat too large. Thus expression (3.10), though being a good estimate to $H(r)$, should be somewhat smaller in the relevant region $r>1.4$. The self-consistency check (2.8) and (4.1) as presented in Fig. 7 reflects these defects.

To more fully appreciate the results of the Onsager-molecule approach we can remark that the degree of accuracy obtained for $g(r)$ using $B_{universal}(r)$ is already comparable to that obtained by solving Eq. (1.2) with the exact bridge function (obtained by computer simulation) for a short-ranged screened Coulomb potential.[18]

TABLE III. Internal energy U (a), and inverse compressibility χ (b), of the 2D OCP. The results correspond to Eq. (1.2) with bridge functions $B=0$ (HNC), $B_{universal}$ [Eq. (2.16)], and B_{OM} [Eq. (2.17) with λ_{OM} given by (3.10)]. The Monte Carlo (MC) results are from Ref. 18.

(a) Internal energy U

Γ	HNC	$B_{universal}$	B_{OM}	MC
1	−0.030	−0.046	−0.058	−0.035
2	−0.278	−0.307	−0.328	−0.288
10	−2.878	−2.972	−3.034	−2.976
20	−6.386	−6.537	−6.626	−6.568
40	−13.579	−13.823	−13.945	−13.876
60	−20.861	−21.184	−21.329	
80	−28.185	−28.581	−28.743	−28.656
100	−35.537	−36.000	−36.169	−36.110
120	−42.907	−43.422	−43.589	−43.524
140	−50.292	−50.825	−50.989	−51.002
160	−57.686	−58.160	−58.372	−58.448
200	−72.500	−72.394		−73.349

(b) Inverse compressibility

Γ	HNC	$B_{universal}$	B_{OM}	Exact
1	0.716	0.930	1.067	0.75
2	0.386	0.806	1.065	0.50
10	−2.815	−0.750	0.353	−1.50
20	−7.254	−3.094	−1.093	−4.00
40	−16.562	−8.145	−4.586	−9.0
60	−26.113	−13.386	−8.439	−14.0
80	−35.785	−18.707	−12.486	−19.0
100	−45.534	−24.072	−16.657	−24.0
120	−55.340	−29.464	−20.927	−29.0
140	−65.186	−34.874	−25.261	−34.0
160	−75.063	−40.293	−29.65	−39.0
200	−94.890	−51.157		−49.0

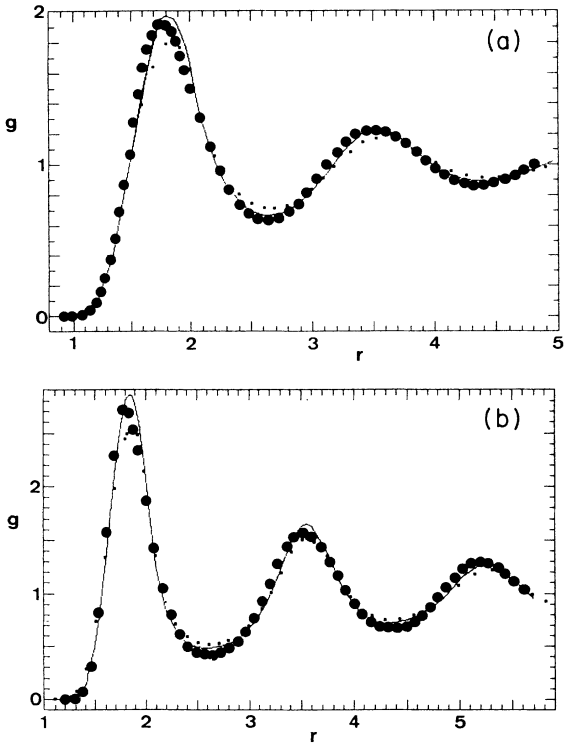

FIG. 6. Radial distribution function $g(r)$, for the 2D one-component plasma. Comparison of the modified HNC calculations using the Onsager-molecule bridge functions $B_{\rm OM}(r)$ (3.10) (solid lines) and $B_{\rm universal}$ (small dots) with the Monte Carlo results (Ref. 18) (closed circles, see text): (a) $\Gamma=40$; (b) $\Gamma=100$.

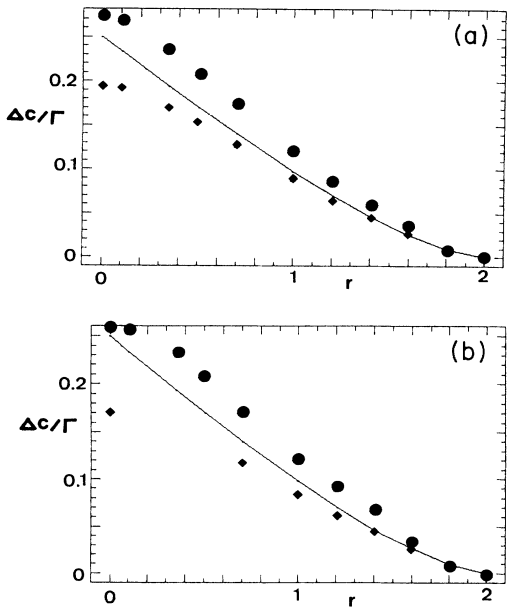

FIG. 7. Modified HNC calculations for the 2D OCP using approximate Onsager-Molecule bridge functions. Deviation $\Delta c(r)/\Gamma$, of the direct correlation function from its asymptotic strong-coupling prediction [check of Eq. (4.1)], for $B_{\rm universal}$ (diamonds) and $B_{\rm OM}(r)$ with $\lambda(r)$ given by (3.10) (closed circles). (a) $\Gamma=100$; (b) $\Gamma=40$.

V. DENSITY PROFILE OF A ONE-COMPONENT PLASMA NEAR A HARD WALL

The density profile of particles in contact with a hard wall can be treated as a limit case of a mixture in which one particle type (the "wall" particle) grows in size and diminishes in concentration.[19] Taking this limit for Eq. (2.8) properly generalized to mixtures (see, e.g., Ref. 7), the universal component ($\lambda=1$) of the wall-particle bridge function is expressed through the fraction of the particle's volume outside the wall when its center is at distance z from the wall. Specifically, for an OCP confined to the region $z>0$ against a wall at $z=0$ we obtain[7]

$$\omega_{\text{wall-particle}}(z) = \begin{cases} 1-3[(z+1)/2]^2+2[(z+1)/2]^3, & z\le 1 \\ 0, & z\ge 1 \end{cases} \tag{5.1}$$

and

$$B_{\text{wall-particle}}(z)=\lambda(z)(\Gamma/5)\omega_{\text{wall-particle}}(z)\ , \tag{5.2}$$

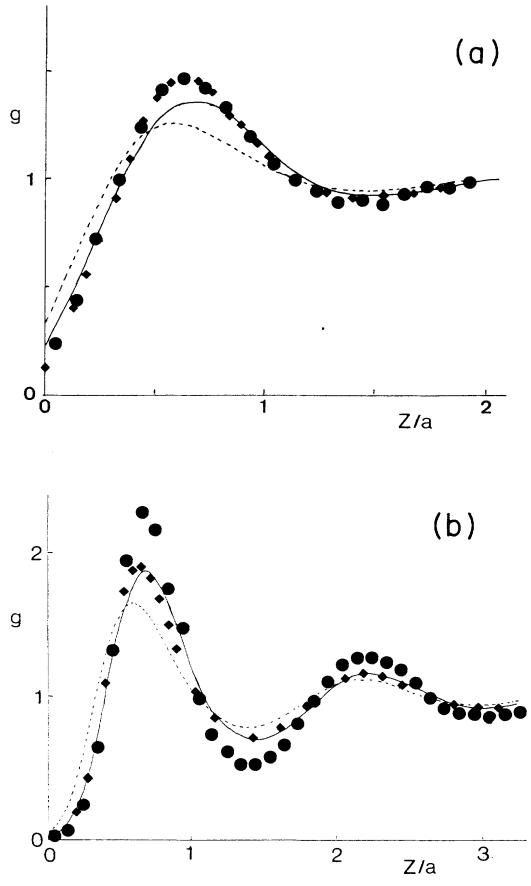

FIG. 8. Density profile of a 3D OCP in contact with a hard wall. Dashed line, $B=0$ (HNC); solid line, $B_{\rm universal}$ [Eq. (5.2) with $\lambda=1$]; diamonds, bridge function from Eqs. (5.2) and (5.3); closed circles, Monte Carlo results (Ref. 19). (a) $\Gamma=10$, $A=1.7$; (b) $\Gamma=30$, $A=0.9$.

where we note that the value of q, $\frac{1}{5}$, is unchanged from its bulk value.[7,20] The MHNC equation has been solved for the density profile along the lines described in Ref. 19 (HNC case) for constant values for λ ranging from 1 (i.e., $B_{\text{universal}}$) to 1.7 and also for the choice

$$\lambda(z)=A(1-z)\ , \tag{5.3}$$

which mimics the behavior of the bulk case in the region $r>1$ (cf. Fig. 1).

The results are summarized in Fig. 8 and compared with HNC results and Monte Carlo simulations.[19] At $\Gamma=10$ the value $A=1.7$ gives a very good overall agreement with the simulation data.[19] At $\Gamma=30$ we could not reach values of A beyond 0.9 because the contact value of $g(z)$ comes very close to zero (as it should) and convergence problems were encountered in the numerical solution of the MHNC equation.

As noted for the bulk case the use of $B_{\text{universal}}$ already considerably improves upon the HNC result of $\lambda=0$. In particular, the peak positions agree much better with the Monte Carlo simulations though there remain substantial differences in the amplitude of the oscillations. When comparing with the simulation results of Ref. 19 one should bear in mind that the latter pertain to the peculiar boundary conditions of a OCP confined to a spherical cavity. It has been argued[21] that these results may be affected by curvature effects even for system sizes of the order of 1000 particles.

The results of $B_{\text{universal}}$ already compare well with the (nonrescaled) results of Ballone *et al.*[21] using appropriate hard-sphere bridge functions. Incidentally, we remark that their rescaling, which yields results comparable to (5.3), should be physically interpreted by the "shift parameter" measuring the position of the wall in the reference hard-sphere system relative to that in the given system.[20]

VI. CONCLUSION

In this work we used the Onsager-molecule approach to calculate the pair structure of various strongly coupled plasmas. We demonstrated that it can be calculated very accurately by employing only the leading term in the strong-coupling expansion of the bridge function around the ideal Onsager state:

$$B(r,\Gamma)=[\lambda_{\text{OM}}(r)q\omega(r)]\Gamma+B_1(r)\Gamma^{\delta}+\cdots\ . \tag{6.1}$$

The correction terms, probably led by a Γ^{δ} term with[9] $\frac{1}{2}\geq\delta\geq\frac{1}{4}$, contain the long-ranged contributions to the otherwise short-ranged [$B_{\text{OM}}(r\geq 2)=0$] leading term. These corrections are of the order of the entropic contributions to the free energies involved in (2.9), which are relatively small in comparison to the corresponding potential-energy terms in strong coupling. Nevertheless, they may be responsible for glassy-state features in the pair correlations.[22] As already discussed in Ref. 7, the present result is in complete accord with the modified HNC theory based on the empirical Percus-Yevick bridge functions for hard spheres, $B_{\text{PYHS}}(r,\eta)$, and an *imposed* thermodynamic consistency for determining the free parameter, $\eta(\Gamma)$. The resulting $B_{\text{PYHS}}(r,\Gamma)$ features the long-range oscillatory behavior, yet

$$B_{\text{PYHS}}(r,\Gamma)/\Gamma\rightarrow 0.2\omega(r)$$

for $\Gamma\rightarrow\infty$.

The Onsager-molecule approach is based on the correspondence between the asymptotic $\Gamma\rightarrow\infty$ properties of the MHNC integral equation for nonsingular bridge functions and the Onsager state. This correspondence was established using the functional derivation of Eqs. (1.1) and (1.2) and physically plausible arguments.[7-9] This implies that in the limit $\Gamma\rightarrow\infty$ the pair potential ϕ and the direct correlation function c are related by

$$\beta\phi(r)\xrightarrow[\Gamma\rightarrow\infty]{\text{HNC}}c(r)=-\beta\Psi(r)\ , \tag{6.2}$$

$$\beta\phi(r)+B_{\text{OM}}(r)\xrightarrow[\Gamma\rightarrow\infty]{\text{MHNC}}c(r)=-\beta\Psi(r)-\beta B_{\text{universal}}(r)\ , \tag{6.3}$$

i.e., a change in the *input* potential that contains the *energy of the Onsager molecule* [i.e., $B_{\text{om}}(r)$] gives rise to a change in the *output* direct correlation function which is given by the *overlap volume function* [i.e., $B_{\text{universal}}(r)$]. The first relation (6.2) was extensively checked[9] numerically with the help of the results of the linearized theory, namely, the mean-spherical model. The second relation (6.3) can be checked via the consistency condition (4.1) when carried to sufficiently large values of Γ. However, for this test to be conclusive Γ must not be too large: due to the increasingly larger exclusion region in $g(r)$, $B(r)$ will be sampled over a smaller and smaller range of r values (eventually only at values close to $r=2$). Thus the range of Γ's near freezing represents a good compromise between the required large Γ's and the required accuracy of the results. In this respect, Fig. 3 represents the best numerically meaningful numerical test that can be performed in three dimensions, with results and trends that certainly speak in favor of the soundness of Eqs. (6.2) and (6.3). The higher sensitivity of the MHNC input-output relation in two dimensions suggests that a somewhat more stringent test could probably be performed as soon as accurate calculations of $u_{\text{OM}}(r)$ in two dimensions will be available.

In conclusion, the Onsager state provides, via the Onsager-molecule approach, an ideal reference point for deriving and analyzing correlations in dense plasmas. Although at an unphysical point, which corresponds to the confined-atom Thomas-Fermi theory, it is still a very useful starting point to attain the physical fluid region.

ACKNOWLEDGMENTS

This research was supported in part by the Fund for Basic Research administered by the Israel Academy of Science and Humanities. The Laboratoire de Physique Theorique et Hautes Energies is Laboratoire Associé au Centre National de la Recherche Scientifique.

[1]J. Pl Hansen and I. R. McDonald, *Theory of Simple Liquids,* 2nd ed. (Academic, New York, 1986).
[2]S. M. Foiles and N. W. Ashcroft, Phys. Rev. A **24**, 424 (1981).
[3]Y. Rosenfeld and N. W. Ashcroft, Phys. Rev. A **20**, 1208 (1979); Phys. Lett. **73A**, 31 (1979).
[4]F. Lado, S. M. Foiles, and N. W. Ashcroft, Phys. Rev. A **28**, 2374 (1983).
[5]J. Talbot, J. L. Lebowitz, E. M. Waisman, D. Levesque, and J. J. Weis, J. Chem. Phys. **85**, 2187 (1986).
[6]Y. Rosenfeld, Phys. Rev. A **29**, 2877 (1984); J. Stat. Phys. **42**, 427 (1986).
[7]Y. Rosenfeld, Phys. Rev. A **37**, 3403 (1988).
[8]Y. Rosenfeld, Phys. Rev. A **35**, 938 (1987); in *Strongly Coupled Plasma Physics,* edited by F. J. Rogers and H. E. DeWitt (Plenum, New York, 1987).
[9]Y. Rosenfeld, Phys. Rev. A **25**, 1206 (1982); **32**, 1834 (1985); **33**, 2025 (1986).
[10]Y. Rosenfeld and L. Blum, J. Phys. Chem. **89**, 5149 (1985); J. Chem. Phys. **85**, 1556 (1986); Y. Rosenfeld and W. M. Gelbart, *ibid.* **81**, 4574 (1984).
[11]B. Widom, J. Chem. Phys. **39**, 2808 (1963).
[12]J. Stein, D. Shalitin, and Y. Rosenfeld, Phys. Rev. A **37**, 4854 (1988).
[13]K. C. Ng, J. Chem. Phys. **61**, 2680 (1974).
[14]W. L. Slattery, G. D. Doolen, and H. E. DeWitt, Phys. Rev. A **21**, 2087 (1980); **26**, 2255 (1982).
[15]H. Totsuji and Wakabayashi, Phys. Rev. A **36**, 4511 (1987).
[16]J. D. Talman, J. Comput. Phys. **29**, 35 (1978).
[17]J. P. Hansen and D. Levesque, J. Phys. C **14**, 603 (1981).
[18]J. M. Caillol, D. Levesque, J. J. Weis, and J. P. Hansen, J. Stat. Phys. **28**, 325 (1982).
[19]J. P. Badiali, M. L. Rosinberg, D. Levesque, and J. J. Weis, J. Phys. C **16**, 2183 (1983).
[20]Y. Rosenfeld and L. Blum, J. Chem. Phys. **85**, 2197 (1986).
[21]P. Ballone, G. Pastore, and M. P. Tosi, Physica A **128**, 631 (1984).
[22]S. Ichimaru and S. Tanaka, Phys. Rev. Lett. **56**, 2815 (1986).